

Recent change of the global monsoon precipitation (1979–2008)

Bin Wang · Jian Liu · Hyung-Jin Kim ·
Peter J. Webster · So-Young Yim

Received: 13 August 2011 / Accepted: 5 December 2011 / Published online: 25 December 2011
© The Author(s) 2011. This article is published with open access at Springerlink.com

Abstract The global monsoon (GM) is a defining feature of the annual variation of Earth's climate system. Quantifying and understanding the present-day monsoon precipitation change are crucial for prediction of its future and reflection of its past. Here we show that regional monsoons are coordinated not only by external solar forcing but also by internal feedback processes such as El Niño-Southern Oscillation (ENSO). From one monsoon year (May to the next April) to the next, most continental monsoon regions, separated by vast areas of arid trade winds and deserts, vary

in a cohesive manner driven by ENSO. The ENSO has tighter regulation on the northern hemisphere summer monsoon (NHSM) than on the southern hemisphere summer monsoon (SHSM). More notably, the GM precipitation (GMP) has intensified over the past three decades mainly due to the significant upward trend in NHSM. The intensification of the GMP originates primarily from an enhanced east–west thermal contrast in the Pacific Ocean, which is coupled with a rising pressure in the subtropical eastern Pacific and decreasing pressure over the Indo-Pacific warm pool. While this mechanism tends to amplify both the NHSM and SHSM, the stronger (weaker) warming trend in the NH (SH) creates a hemispheric thermal contrast, which favors intensification of the NHSM but weakens the SHSM. The enhanced Pacific zonal thermal contrast is largely a result of natural variability, whilst the enhanced hemispherical thermal contrast is likely due to anthropogenic forcing. We found that the enhanced global summer monsoon not only amplifies the annual cycle of tropical climate but also promotes directly a “wet-gets-wetter” trend pattern and indirectly a “dry-gets-drier” trend pattern through coupling with deserts and trade winds. The mechanisms recognized in this study suggest a way forward for understanding past and future changes of the GM in terms of its driven mechanisms.

This paper is a contribution to the special issue on Global Monsoon Climate, a product of the Global Monsoon Working Group of the Past Global Changes (PAGES) project, coordinated by Pinxian Wang, Bin Wang, and Thorsten Kiefer.

B. Wang
Department of Meteorology, University of Hawaii at Manoa,
Honolulu, HI 96825, USA

B. Wang · S.-Y. Yim
International Pacific Research Center, University of Hawaii
at Manoa, Honolulu, HI 96825, USA

J. Liu (✉)
State Key Laboratory of Lake Science and Environment,
Nanjing Institute of Geography and Limnology, Chinese
Academy of Sciences, 73 East Beijing Road,
Nanjing 210008, China
e-mail: jianliu@niglas.ac.cn

H.-J. Kim
Research Institute for Global Change,
Japan Agency for Marine-Earth Science and Technology,
3173-25 Showa-machi, Kanazawa-ku, Yokohama,
Kanagawa 236-0001, Japan

P. J. Webster
School of Earth and Atmospheric Sciences, Georgia Institute
of Technology, Atlanta, GA 30308, USA

1 Introduction

There is no climate variability that will impose greater impacts on society than changes in monsoon precipitation which exists as the life blood of about two-thirds of the world's population. Precipitation also plays an essential role in determining atmospheric general circulation and hydrological cycle, and in linking external radiative forcing

and the atmospheric circulation. In order to predict the future changes of the global monsoon precipitation (GMP), it is crucial to determine the response of the GMP to the recent global warming.

In physical essence, monsoon is a forced response of the climate system to annual variation of insolation. The annual variation of solar radiation is a fundamental driver and a necessary and sufficient condition for the existence of monsoon. The land–sea thermal contrast is critical for the location and strength of the monsoon but it is neither a necessary nor a sufficient condition. Based on this viewpoint, monsoon must be a global phenomenon. Trenberth et al. (2000) depicted the global monsoon (GM) as the global-scale seasonally varying overturning circulation throughout the tropics. Wang and Ding (2008) have demonstrated that the GM represents the dominant mode of the annual variation of the tropical precipitation and low-level winds, which defines the seasonality of Earth's climate. Thus, the annual variation of all regional monsoons can be viewed as an integrated GM system. In fact, it has been well established that over the last glacial-interglacial transition, the observed changes in regional monsoons are evidently synchronized by known changes in orbital forcing (Kutzbach and Otto-Bliesner 1982; Liu et al. 2004). Such coordinated variations of regional monsoons have also recently shown to occur on centennial-millennial time scales (Liu et al. 2009).

However, studies of monsoon interannual-interdecadal variations have primarily focused on regional scales, e. g., South Asia (e.g., Webster et al. 1998), East Asia (e.g., Tao and Chen 1987), Australia (e.g., McBride 1987), Africa (e.g., Nicholson and Kim 1997), North America (e.g., Higgins et al. 2003), and South America (e.g., Zhou and Lau 1998). It has been a traditional notion that each regional monsoon has indigenous characteristics due to its specific land–ocean configuration and orography and due to differing feedback processes internal to the coupled climate system. Although linkages among various regional monsoons have been noticed (e.g., Meehl 1987; Wang et al. 2001; Lau and Weng 2002; Biasutti et al. 2003), the recent variations of monsoon precipitation have not been studied on a global scale over both land and ocean areas. Besides, prior to the satellite era beginning in 1979 (Wentz et al. 2007), our knowledge of global precipitation variation has been limited to land areas (Dore 2005; Zhang et al. 2007; Wang and Ding 2006). Hitherto little is known about how the GMP has responded to the last three-decade period of rapid global warming.

The present study deals with the GM, the integral of all regional monsoon systems. This broader perspective allows us to view changes in the total system due to anthropogenic effects, very large scale natural long-term oscillations and the influences of major interannual variations [e.g., El Niño–Southern Oscillation (ENSO)]. Only in the context of the GM, can a more holistic overview be made and new

findings revealed. Changes in the regional monsoons (say over India) cannot be fully understood unless we considered within a global perspective.

The primary objective of the present study is to document interannual and decadal variations (or 30-year trends) of the GMP and to understand fundamental drivers for the GMP variability using modern global observation (1979–2008). Efforts are made to address the following specific questions: To what extent can the internal feedback processes drive global-scale monsoon variability? Are there any trends in global-scale monsoons during recent decades? What give rise to the trends, if any? Are there any differences between the northern hemisphere summer monsoon (NHSM) and southern hemisphere summer monsoon (SHSM) variability? What cause the differences, if any? What roles does GM change play in global precipitation change? These questions are discussed in Sects. 4 through 7.

2 Data and methodology

There are two global (land and ocean) precipitation datasets available: Global Precipitation Climatology Project (GPCP, Huffman et al. 2009) and Climate Prediction Center merged analysis of precipitation (CMAP, Xie and Arkin 1997). For description of climatology and interannual variations, an arithmetic mean of the two datasets was used. But to determine the long-term trend we primarily used GPCP data because CMAP is calibrated to atoll gauge data and this calibration may have introduced inhomogeneity in long-term changes (Yin et al. 2004). However, in the post-SSM/I (Special Sensor Microwave/Imager) era (i.e., after 1987) the two datasets tend to have consistent trends and interannual variation on global scale. The circulation data used are also an arithmetic mean dataset, based on National Centers for Environmental Prediction–Department of Energy reanalysis 2 (NCEP2, Kanamitsu et al. 2002) and the European Centre for Medium-Range Weather Forecasts (ECMWF) reanalysis (ERA) which is a combination of the 40-year reanalysis (ERA-40, Uppala et al. 2005) and Interim ERA (1989–2008). Monthly mean sea surface temperature (SST) data were obtained from the National Oceanic and Atmospheric Administration (NOAA) extended reconstructed SST (ERSST) version 3 (Smith et al. 2008). The data periods are from 1979 to 2009 with horizontal resolution of 2.5° except ERSST of which the grid spacing is 2.0°.

Two methods were used to test the significance of linear trends: The trend-to-noise ratio and the nonparametric Mann–Kendall rank statistics (Kendall 1955). The maximum covariance analysis (MCA) (Wallace et al. 1992; Ding et al. 2011) was used to identify important coupled modes of variability between GMP and underlying SST

fields. The empirical orthogonal function (EOF) analysis is used to show the importance of the MCA mode.

3 Definition of GM domain and GMP intensity

Traditionally, the GM domain was determined based on annual reversal of prevailing wind direction and speed (Ramage 1971); the resultant monsoon domains primarily cover tropical eastern hemisphere (30°S–30°N, 20°W–160°E). Recent studies, on the other hand, define monsoon domains in terms of the rainfall characteristics (wet summer vs. dry winter), and the resultant GM domain includes all regional monsoons of South Asia, East Asia, Australia, northern (West) and southern Africa, and North and South America (Fig. 1).

The interannual variation has been conventionally studied based on the calendar year. However, for the analysis of year-to-year GMP variation, use of the calendar-year average is inadequate, because, as shown in Fig. 2, seasonal distribution of GMP has a minimum in April with double peaks occurring in July–August (due to NHSM) and January–February (due to SHSM). In order to depict the interannual variation of annual mean GMP, we use the “global monsoon year” starting from May 1 to the following April 30, which includes the NHSM from May to October followed by the SHSM from November to April next year. Note that this definition is suitable not only for GM but also for depicting ENSO evolution, because ENSO events normally start from May, mature toward the end of the calendar year, and decay in the following boreal spring (Rasmusson and Carpenter 1982).

In this paper, the GMP means the annual mean monsoon precipitation measured for each monsoon year. To reflect the monsoon strength, we use local summer monsoon rainfall, which provides a good measure of the annual range of precipitation because the annual range is dominated by local summer rainfall in monsoon regions. The NHSM precipitation intensity (NHMPI) can be measured by the total monsoon precipitation (or area averaged mean monsoon precipitation rate) in the NH monsoon domain during boreal summer (MJJAS). Similarly, the SHSM precipitation intensity (SHMPI) can be measured by the total monsoon precipitation (or area averaged mean monsoon precipitation rate) in the SH monsoon domain during austral summer (NDJFM). The GMP intensity (GMPI) is, then, defined by the sum of NHMPI and SHMPI.

4 Interannual variations of GMP

To what extent can the interannual variations of GMP be driven by internal feedback processes in the climate system? Figure 3 shows the leading “coupled” mode of the monsoon-year-average GMP and underlying SST fields derived by MCA (hereafter MCA1), which explains about 72% of the total covariance between the two fields and about 24% of the total monsoon rainfall variance. The GMP pattern and evolution in MCA1 are nearly identical to those in the first EOF of GMP with spatial and temporal correlation coefficients of 0.96 and 0.99, respectively (figure not shown). This indicates that the MCA1 also faithfully represents the most important pattern of interannual GMP variability.

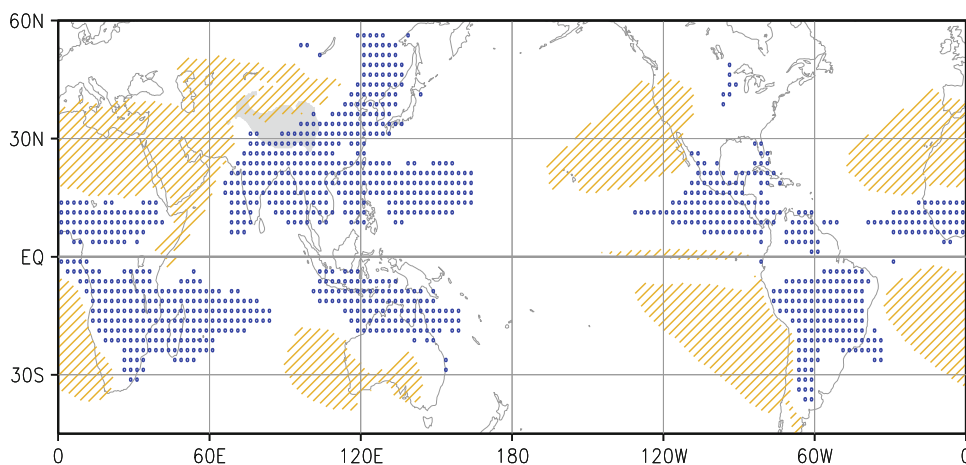


Fig. 1 Global monsoon precipitation domain as defined by the local summer-minus-winter precipitation rate exceeding 2.0 mm/day and the local summer precipitation exceeding 55% of the annual total (stippled, blue). Here the local summer denotes May through September (MJJAS) for NH and November through March (NDJFM)

for SH. The threshold values used here distinguish the monsoon climate from the adjacent dry regions where the local summer precipitation less than 1 mm/day (hatched, yellow) and perennial equatorial climate. The 3,000-m height contour surrounding Tibetan Plateau is shaded. The merged GPCP-CMAP data were used

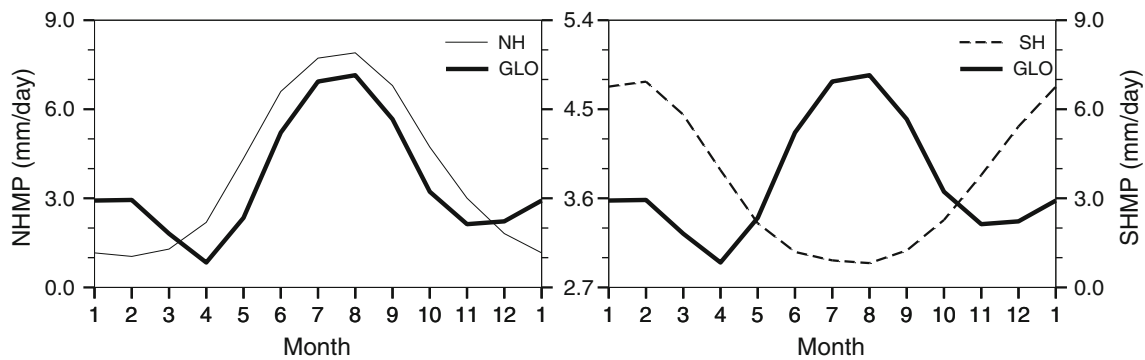


Fig. 2 Climatological annual cycle of precipitation rate (mm/day) averaged over the NH (left) and SH (right) monsoon regions and the globe (thick line with scale at the center). The global monsoon

precipitation (GMP) exhibits an annual minimum in April and double peaks in July–August and January–February. The ensemble mean CMAP and GPCP precipitation dataset was used

The spatial pattern of interannual variation of monsoon precipitation (Fig. 3a) is overwhelmed by suppressed rainfall in majority of regional monsoons except the southwestern Indian Ocean and the southern part of the South American monsoon. In particular, the suppressed precipitation dominates over nearly all continental monsoon regions. The overall drying pattern is associated with a warm phase of ENSO (Fig. 3b). During the development (boreal summer) and mature phases (austral summer) of El Niño episodes, the warming in the eastern-central Pacific displaces the North Pacific intertropical convergence zone and the South Pacific convergence zone equatorward, thereby directly reducing Australian and North American monsoon rainfall (Webster et al. 1998). The suppressed maritime continental precipitation induces anticyclonic anomalies in the off-equatorial South Asian summer monsoon region, suppressing South Asian monsoon rainfall (Wang et al. 2003). El Niño also reduces rainfall over continental Africa and northern South America through atmospheric teleconnections (Enfield 1996; Nicholson and Kim 1997).

Since ENSO is a consequence of the internal ocean–atmosphere feedback processes, the result here suggests that the regional monsoons can be coordinated not only by external forcing on centennial and orbital time scale but also, to a large extent, by internal feedback processes. Results in Fig. 3 also suggest that during the recent three decades, the NHSM is better coordinated by ENSO than the SHSM, because in the southern African and South American monsoon regions, the ENSO-induced precipitation anomalies tend to have a dipolar structure, rather than a uniform pattern (Fig. 3a).

5 The decadal variations and 30-year trends (1979–2008) of GMP

Beyond ENSO time scale, we depict GMP variations using 3-year running mean data. Figure 4 shows the MCA1

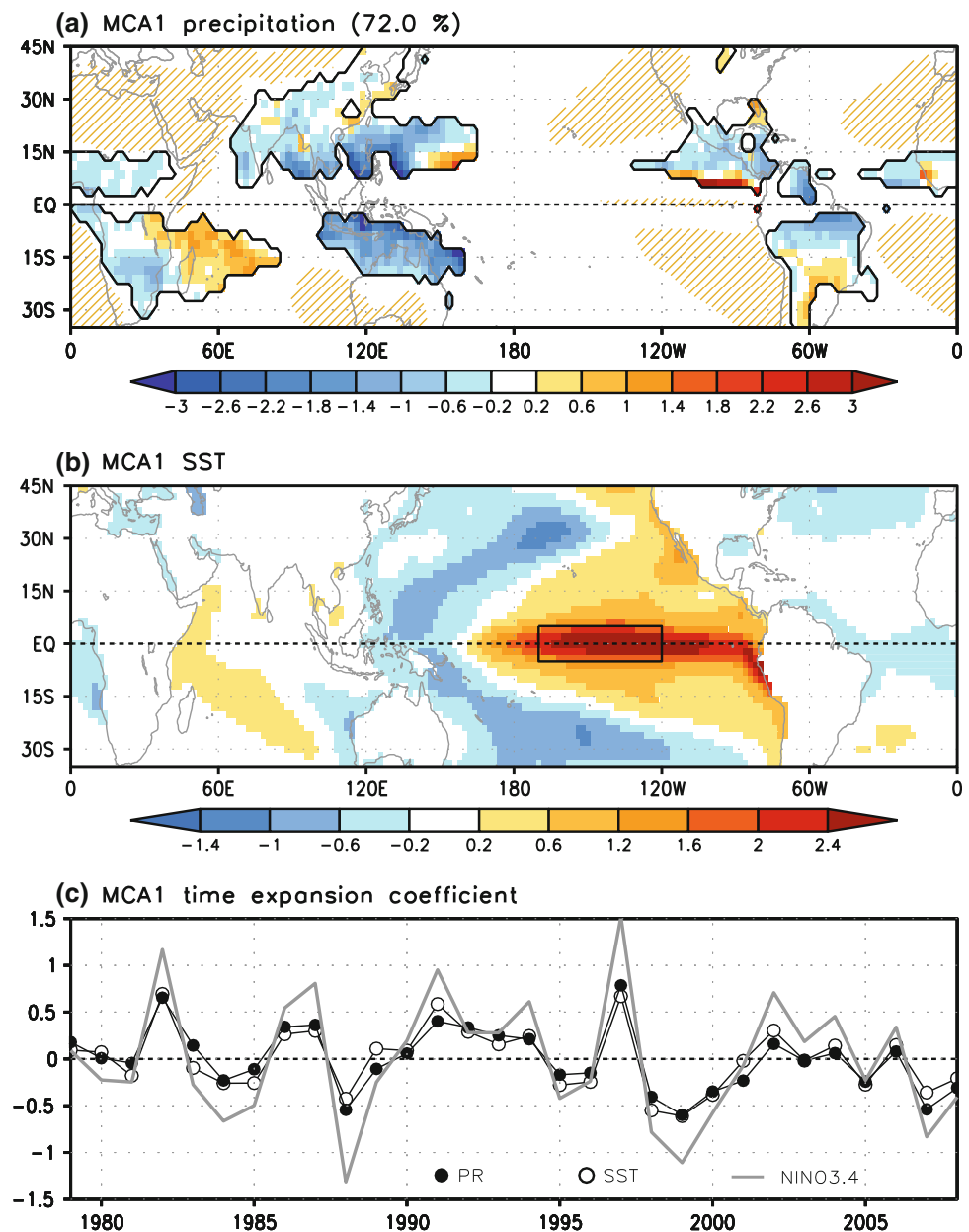
between 3-year running mean GMP and SST, which accounts for about 62% of the total smoothed covariance. The monsoon precipitation shows a predominant increasing trend across different regional monsoons. This decadal trend pattern concurs with rising SSTs in the global ocean except in the eastern Pacific (EP) where cooling trend occurs (Fig. 4b).

A question arises as to whether the decadal trend can be seen in the GMPI which is measured as the area-averaged rate of local summer precipitation falling into all regional monsoon domains. We first note that the GMPI is anti-correlated with the ENSO index ($r = -0.80$). However, the ENSO index has no significant trend. In sharp contrast, both GMPI and NHMPI show an intensifying trend, statistically significant at 95% confidence level (Fig. 5a; Table 1). The total trend in GMPI ($0.07 \text{ mm day}^{-1} \text{ decade}^{-1}$) is slightly weaker than that in the NHMPI ($0.08 \text{ mm day}^{-1} \text{ decade}^{-1}$) because the SHMPI has a weak and insignificant upward trend (Table 1). Note also that the GPCP and CMAP data are more homogeneous and reliable after the mid-1987 when a large amount of SSM/I data were used for estimation of oceanic rainfall (Huffman et al. 2009). During the post-SSM/I era (last 20 years) both the GPCP and CMAP datasets exhibit consistent and significant upward trends in the GMPI (Fig. 5b). In addition, in the post-SSM/I era the over-ocean and over-land components of the GMPI exhibit cohesive interannual variation and trends (Fig. 5c).

6 Cause of the recent GMP change

To understand the cause of the increasing trend in GMPI, a starting point is to consider the recent global warming effect, which increases moisture contents and hence enhances precipitation, including monsoon rainfall. However, the processes controlling monsoon rainfall change is far more complex than this simple thermodynamic

Fig. 3 The leading coupled mode of monsoon-year mean precipitation in global monsoon domains and the corresponding global SST derived by maximum covariance analysis which explains about 72% of the total covariance. Spatial patterns of monsoon precipitation (a) and SST (b) are shown together with their corresponding time expansion coefficients (c). For comparison, the Niño 3.4 SST anomaly (an ENSO index averaged over the box inserted in b) averaged over the monsoon years are also shown in the lower panel. The GMP domain and the arid regions are defined in Fig. 1. The merged GPCP-CMAP data ERSST were used



argument. It is important to account for the spatial and temporal structure of the change.

To better understand what drives the increased GMPI, we first examine the trend pattern of SST (Fig. 6a) because it reflects changes in the lower boundary condition. The SST trend is essentially the same as the decadal variation pattern shown in Fig. 4b. A salient feature in Fig. 6a is a cooling in the EP and a contrasting warming in the western Pacific (WP). Can this zonal temperature gradient contribute to GMPI variability and trend?

To address this question, we represent this broad scale east–west asymmetry in Pacific SST by a zonal SST gradient index (ZSSTGI),

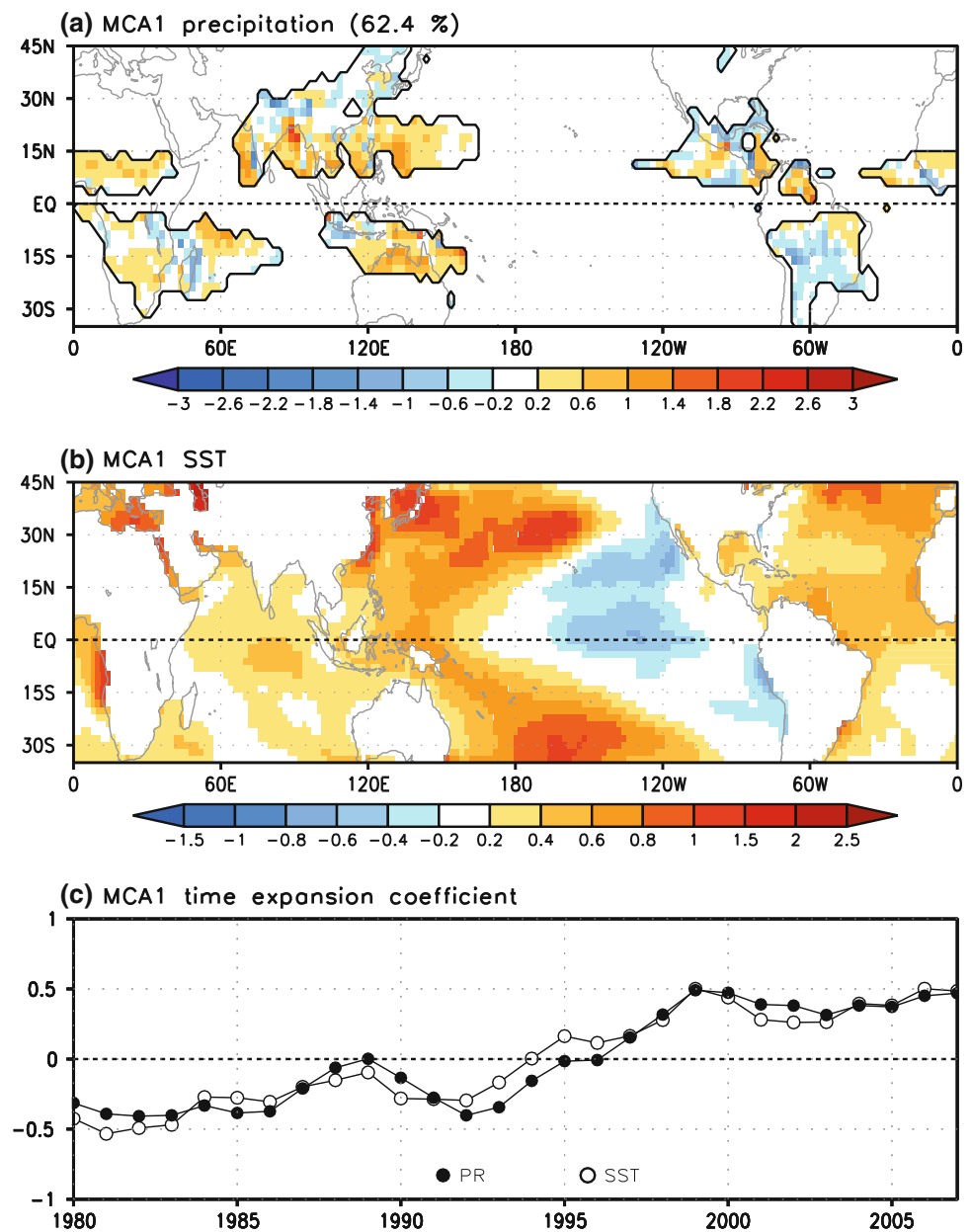
$$\text{ZSSTGI} = \text{SST} (20^{\circ}\text{S}–20^{\circ}\text{N}, 160^{\circ}\text{W}–80^{\circ}\text{W}) - \text{SST} (40^{\circ}\text{S}–40^{\circ}\text{N}, 120^{\circ}\text{E}–160^{\circ}\text{W}).$$

The corresponding SLP trend features a rising SLP in the Pacific east of the dateline and lowering SLP in the eastern hemisphere tropics and even the tropical Atlantic (Fig. 6b). To depict this east–west asymmetry in SLP trend field, we define an Indo-Pacific zonal oscillation index (ZOI),

$$\text{ZOI} = \text{SLP} (40^{\circ}\text{S}–40^{\circ}\text{N}, 160^{\circ}\text{W}–110^{\circ}\text{W}) - \text{SLP} (20^{\circ}\text{S}–20^{\circ}\text{N}, 50^{\circ}\text{E}–150^{\circ}\text{E}).$$

The time series of ZSSTGI and ZOI are shown in Fig. 6c. Both have large interannual fluctuations which are

Fig. 4 a–c The same as Fig. 3 except for using 3-year running mean datasets of GPCP and ERSST



associated with ENSO on the interannual time scale. Nevertheless, both time series show significant trends (Table 2). The enhanced trend of “EP cooling-WP warming” across the Pacific induces rising SLP in the EP where the two subtropical Highs straddle the equator. This, in turn, enhances the trades, transporting and converging moisture into the eastern hemisphere monsoon regions in particular, thereby leading to the increased GMPI. Thus, the “EP cooling-WP warming” mechanism favors intensification of the GMP on both the interannual and multi-decadal time scale (trend).

The 30-year trend in GMPI associated with the “EP cooling-WP warming” trend could be part of multi-decadal variations. Over the Pacific domain, the SST patterns in

Figs. 4b and 6a resemble the interdecadal Pacific oscillation (IPO) (Power et al. 1999; Deser et al. 2004). Note that the IPO and long-term warming trend are two different modes. Figure 7 presents the first two EOF modes of SST variation during a longer period (1950–2010). The first EOF represents a long-term global warming trend, whereas the second EOF depicts the IPO. The SST trend patterns in Figs. 4b and 6a are akin to the EOF2 spatial pattern, indicating that they don’t belong to the long-term global warming trend that corresponds to EOF1.

To what extent does the global warming contribute to GMP change during the past 30 years? To address this question we examine the 2 m air temperature (T2) trend pattern (Fig. 8). There are two prominent characteristics in

Fig. 5 Recent amplification of NH and global summer monsoon. **a** Time series (1979–2008, monsoon year) of NH summer monsoon precipitation intensity (NHMPI) and GMP intensity (GMPI). The intensity is defined by the area-weighted mean local summer monsoon precipitation rate (mm/day). The GPCP dataset was used. The *thick gray lines* indicate linear trends (see Table 1 for the significance of the trend). **b** Time series (1989–2008) of GMPI derived from both GPCP and CMAP. **c** Time series (1989–2008) of the land and ocean components of the GMPI obtained from GPCP. In **b** and **c**, the linear trends are significant at 95% confidence level or higher by the trend-to-noise ratio test and the Mann–Kendall rank statistics

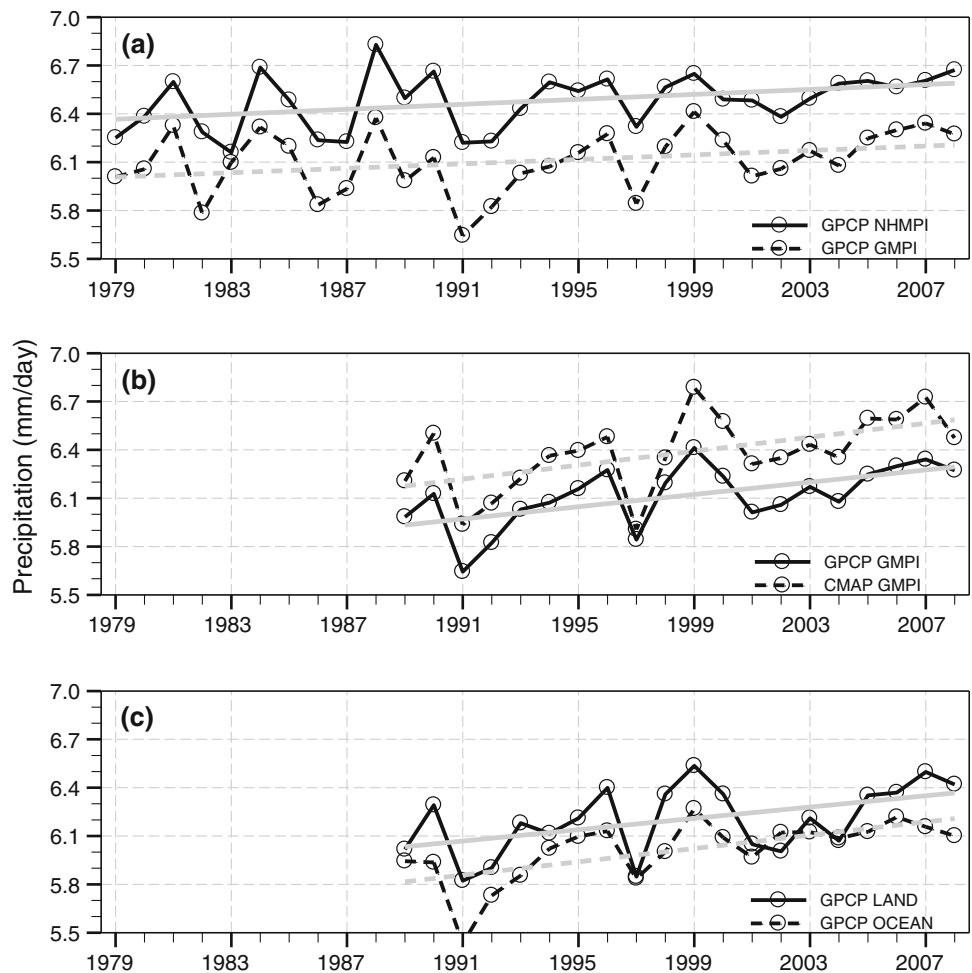


Table 1 Monsoon precipitation intensity trends (in units of mm day⁻¹ decade⁻¹) and the statistical significance levels for the trend-to-noise ratio (T2N) and Mann–Kendall rank statistics (MK) tests

NHMPI			SHMPI			GMPI		
MK	T2N	Trend	MK	T2N	Trend	MK	T2N	Trend
95	95	0.08	–	–	0.06	95	90	0.07

The trends are calculated from 30-year (1979–2008) GPCP data. Area-weighting was applied

T2 trend, i.e., the land areas are warmer than oceanic areas and the NH is warmer than the SH. The former arises from the fact that the ocean warms slower than land because of a higher heat capacity and an ability to mix heat downward. The latter is related to the former and the fact that the NH has more land areas than the SH. As a result, the global land-minus-ocean temperature has a significant trend of 0.13°C per decade (Fig. 8b; Table 2), which contributes to the vigor of the global monsoon. Note, however, the enhanced land–ocean thermal contrast prevails in the NH but not in the SH (Fig. 8a), suggesting that this factor is primarily intensifies the NHSM. Further, the NH surface warming trend is much greater than the SH warming trend (Fig. 8c), which generates cross-equatorial pressure gradients that drive low-level

cross-equatorial flows from the SH to the NH, strengthening NH monsoon (Loschnigg and Webster 2000). Thus, the combined effects of the land–ocean and NH–SH thermal contrasts yield a strong intensification in the NH monsoon. On the other hand, the NH–SH contrast exerts an opposing effect on the SHSM, offsetting the positive contribution of other contributing processes (such as the EP cooling-WP warming trend discussed above), leading to a weak trend in SH monsoon. The stronger interannual variation during the austral summer might also weaken the signal of the long-term SHSM trend (Chou et al. 2007). As such, the “warm land-cold ocean” and “warm NH-cold SH” mechanisms can explain why the NHMPI has a strong upward trend, while SHMPI has a weaker trend. Since about 61% of the GMPI is

Fig. 6 Linear trend (1979–2008) maps of **a** ERSST (°C) and **b** sea-level pressure (SLP). The SLP was derived from the ensemble mean ERA and NCEP2 reanalysis. Stippling regions indicate statistical significance at 90% level or higher by the trend-to-noise ratio. The *square areas* denote the regions where zonal SST gradient and SLP difference are defined. **c** Zonal SST gradient (*red* with scale on the *left*) and Indo-Pacific zonal oscillation indices (*blue* with scale on the *right*) along with their trends (*dashed lines*). A calendar-year mean was used

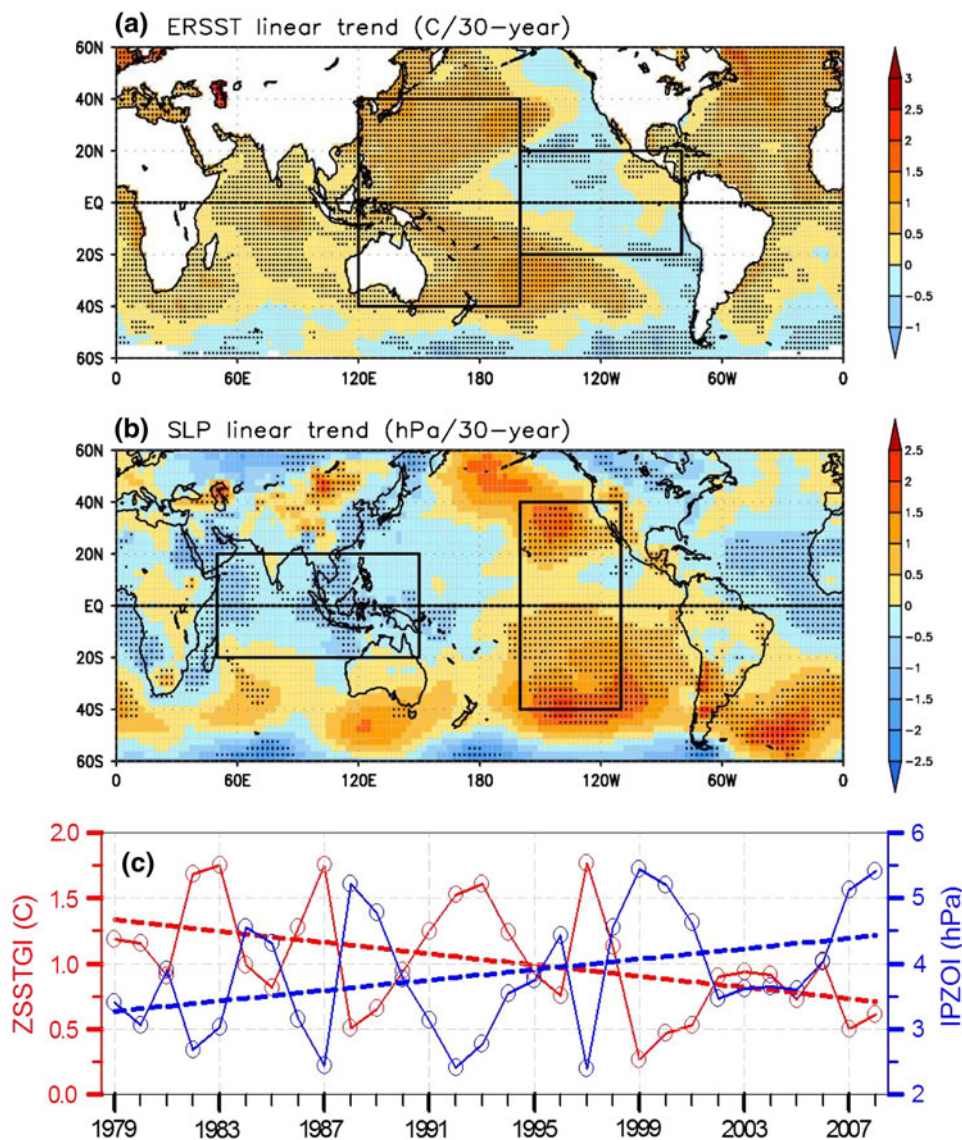


Table 2 Trends (1979–2008) of land-minus-ocean T2, NH-minus-SH T2, zonal SST gradient index (ZSSTGI), and Indo-Pacific zonal oscillation index (ZOI) and their confidence levels determined by the trend-to-noise ratio (T2N) test

	Trend (decade ⁻¹)	T2N
Land-minus-ocean T2 (°C)	0.13	99
Hemispheric T2 (°C)	0.12	99
ZSSTGI (°C)	-0.21	-95
ZOI (hPa)	0.40	95

determined by the NHMPI, the GMPI has also a significant upward trend over the past 30 years.

Based on the above analysis, we suggest that the recent trend of GMPI is attributed to both natural variability and anthropogenic forcing. The “EP cooling-WP warming” largely arises from an internal feedback processes, because

the Intergovernmental Panel on Climate Change (IPCC) Fourth assessment report (AR4) shows that the majority of the model project an EP warming or so-called El Nino-like global warming under increasing greenhouse gases forcing (Meehl et al. 2007; Fig. 9). On the other hand, the increasing land–ocean and inter-hemispheric thermal gradients are likely a consequence of the anthropogenic forcing because the projected future temperature change shows a robust warm NH-cold SH and warm land-cold ocean warming pattern (Chou et al. 2007).

7 Impact of GMP amplification on global precipitation change

The enhanced GMP may produce a “wet-gets-wetter” and “dry-gets-drier” trend pattern in the global annual mean

Fig. 7 The first (left) and second (right) EOF modes of ERSST for the period 1950–2010. The EOF1 represents a long-term trend and the EOF2 reflects the interdecadal Pacific oscillation (IPO) pattern. The 3-year running mean was used

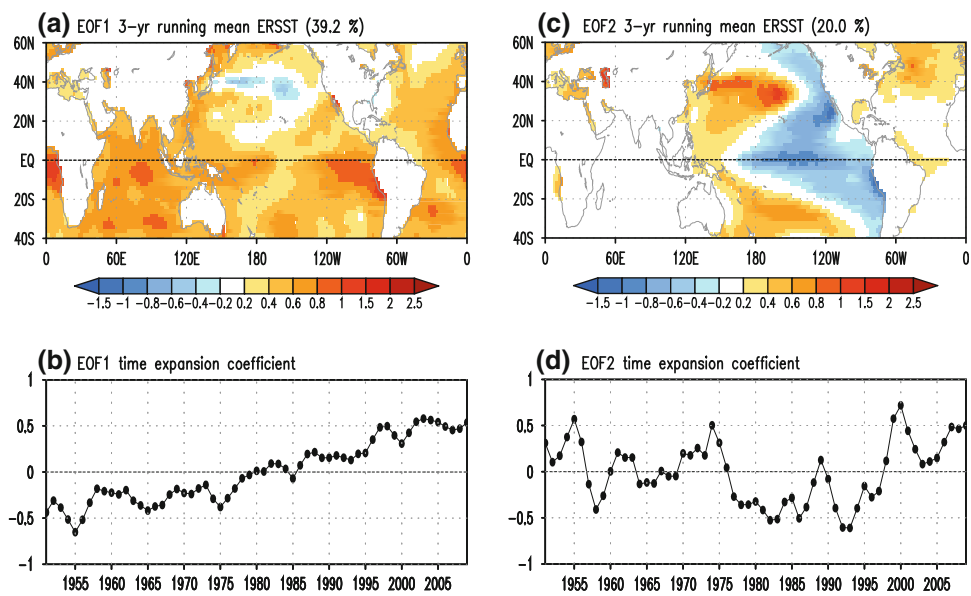
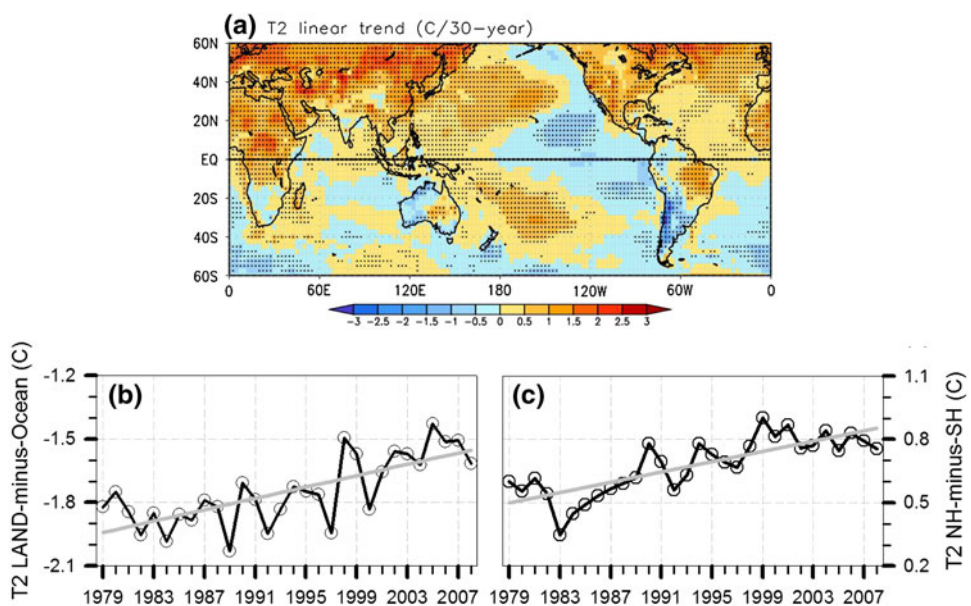


Fig. 8 a Linear trend (1979–2008) maps of 2-m air temperature (°C). Stippling regions indicate statistical significance at 90% level or higher by the trend-to-noise ratio. b Time series of “land minus ocean” T2 difference. The land and ocean components were area mean values averaged between 40°S and 40°N. c The same as in b except for the “NH minus SH” T2 difference. Here, the ensemble mean of ERA and NCEP2 reanalysis averaged over a calendar year was used



precipitation. Figure 10a indicates that over the past 30 years precipitation has increased within the climatological ‘wet’ regions and decreased in the relatively ‘dry’ regions. Overall, these trend patterns resemble the ‘rich-gets-richer’ pattern recognized from multi-model projections of climate change (Neelin et al. 2006). The precipitation response to global warming is a complex process (Held and Soden 2006) and not fully understood. We hypothesize that an intensified GMP contributes to the ‘wet-gets-wetter’ global precipitation trend pattern. This is supported by the fact that the local summer precipitation trend bears a close resemblance to the annual precipitation trend (Fig. 10b). As shown in Fig. 10b, the summer monsoon rainfall shows a general increasing trend across the

majority of the regional monsoon regions except the South American monsoon. In contrast to an enhanced global local summer monsoon precipitation, most arid and semiarid desert or trade wind regions, located to the west and poleward of each monsoon region, show drying trends (Fig. 11a). The precipitation in dry regions not only has an opposite trend to the GMPI but also tends to be anti-correlated with it on interannual time scale ($\gamma = -0.34$). This anti-correlation between the monsoon and desert is more evident in the NH ($\gamma = -0.42$) (Fig. 11b). Hence, the ‘dry-gets-drier’ pattern may be rooted in the intensification of the monsoon-desert coupled system. Note, however, that these negative correlations tend to be weakened after removal of the linear trend.

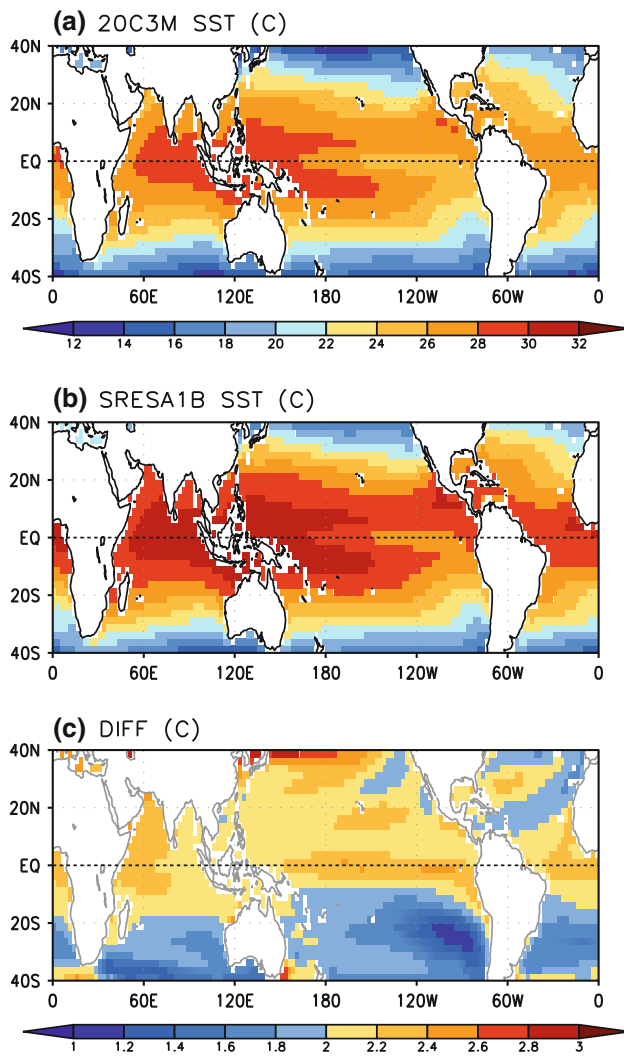


Fig. 9 Mean SST field for **a** present day (PD) period (1970–1999), **b** the global warming (GW) period (2070–2099), and **c** the changes in SST (GW minus PD). The PD and GW SSTs are derived from the 20C3M and SRESA1B simulations of 22 coupled global climate models that participated in the World Climate Research Program/ Coupled Model Inter-comparison Project 3 (CMIP3)

The monsoon-desert coupling mechanism is arguably an important dynamic factor in formation of the wet-gets-wetter and dry-gets-drier trend pattern in the total global precipitation. The drying trend in the arid regions results from the increased descent produced by the monsoon heating-induced Rossby waves that interact with subtropical westerly flows (Hoskins 1996). This monsoon-westerly interaction mechanism is illustrated in Fig. 12a. The diabatic heating in the monsoon region induces a Rossby-wave pattern to the west. This has an anticyclone at upper levels and a cyclone at lower levels. From hydrostatic balance there must be warmth in the mid-troposphere, thus a deepening of the isentropic surface. When this thermal structure is far enough poleward to interact with the

southern flank of the mid-latitude westerlies, the air moves down the isentropes on their western side and backs up on their eastern side (Hoskins and Wang 2006). Trajectories indicate that the monsoon-desert mechanism does not represent a simple ‘Walker-type’ overturning cell. Instead, the descending air is seen to be mainly of mid-latitude origin. Over the desert regions, the descending motion can be further reinforced by local longwave radiative cooling which in turn strengthens a secondary circulation between the monsoon and desert, i.e., the transverse circulations (Webster et al. 1998). Over oceanic subtropical high regions (such as the EP) the descent induced by monsoon-westerly interaction can be further enhanced by air–sea interaction over the trade wind oceans (Rodwell and Hoskins 2001). As shown in Fig. 12b, a percentage of descent in the North Pacific subtropical anticyclone off California could come from a positive feedback involving air–sea interaction. Off the coast of Baja California along shore northwest winds prevail in the intense eastern portion of the subtropical High. These equatorward winds result from the vortex shrinking accompanying the Mexican monsoon-induced descent, according to the Sverdrup balance. On the other hand, the equatorward along-shore wind stress will lead to offshore Ekman transport (Anderson and Gill 1975), inducing oceanic upwelling, and leading to cold SSTs. The decreased surface temperature, in turn reinforces the suppression of convection through changes to the moist static energy (Neelin and Held 1987) and the formation of marine stratus clouds. Below the descending motion and associated with it lies the vast marine stratus cloud deck, which, owing to its persistence, low altitude and high reflectivity, in turn enhances the local longwave radiative cooling at the stratus cloud top. The effects of radiative cooling could enhance the descending motion and seem to be a very important contributor to the enhancement of the subtropical anticyclone.

8 Summary

We have demonstrated that internal feedback processes such as ENSO can cause a coherent variation among various regional monsoons, especially over the continental monsoon regions (Fig. 3). Therefore, regional monsoons are coordinated not only by external forcing on the diurnal, annual (Wang and Ding 2008), orbital (Liu et al. 2004), and centennial-millennial (Liu et al. 2009) time scales, but also by internal feedback processes and atmospheric teleconnections. This result also implies that the change of ENSO properties in the past [such as a permanent El Niño reported by Wara et al. (2005)] may induce monsoon changes on the globe scale.

Fig. 10 Recent trends (1979–2008) in **a** global annual precipitation and **b** precipitation in summer monsoon season (i.e., MJJAS for NH and NDJFM for SH) in units of $\text{mm day}^{-1} \text{ decade}^{-1}$. The significance of the linear trends was tested using the trend-to-noise ratio. Areas passing 90% confidence level were stippled. The GPCP data were used. In **a** the climatological annual mean precipitation rate was shown by contours (1 (red), 2 (blue), 4, and 8 (purple) mm/day). In **b** the monsoon and desert regions as defined in Fig. 1 were delineated by blue and red, respectively

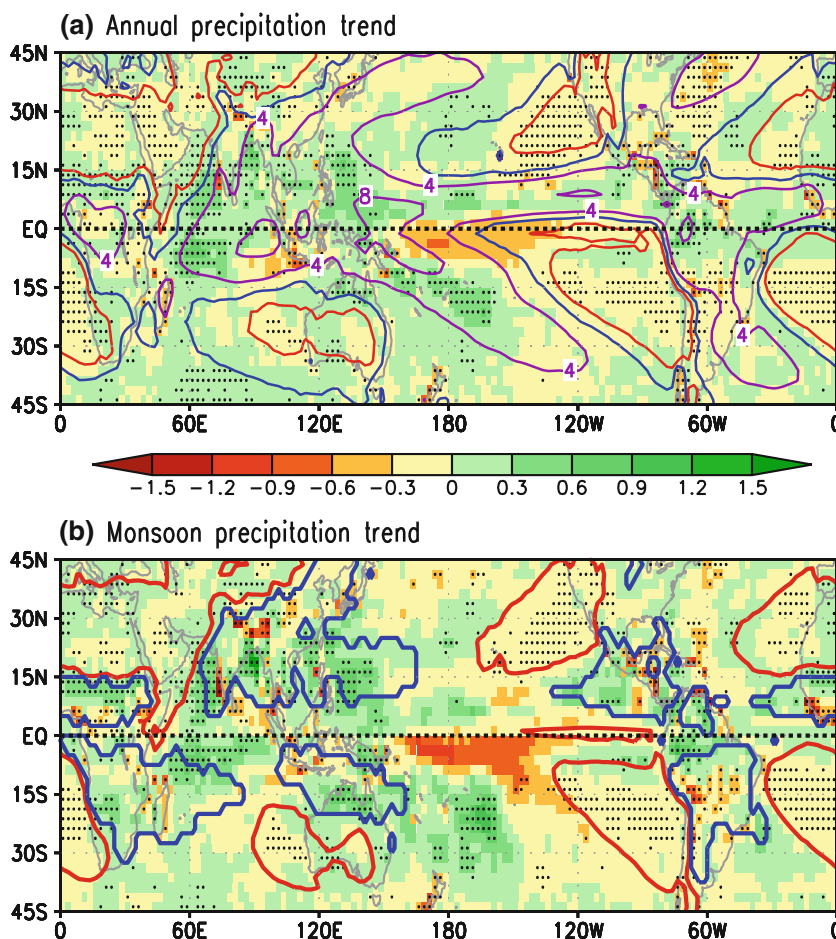
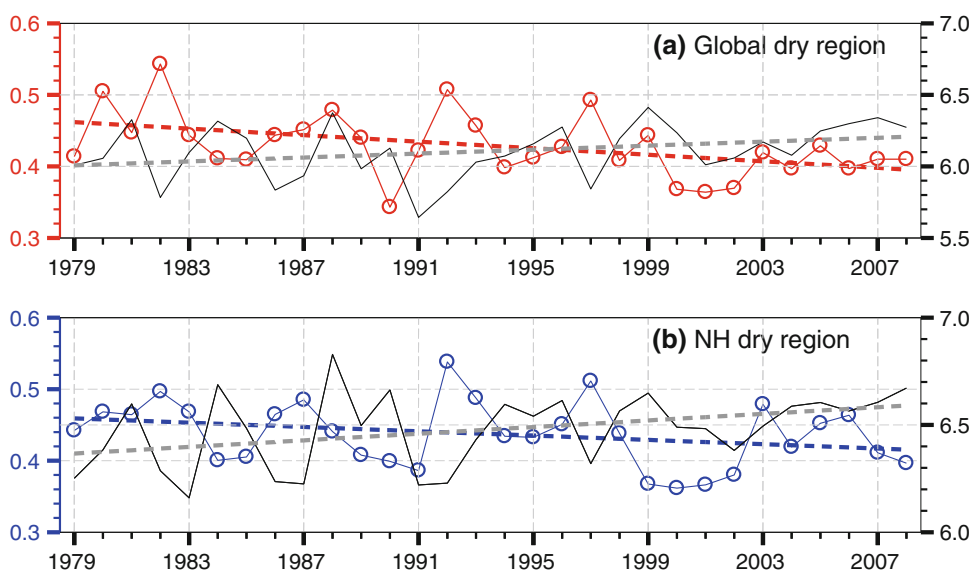


Fig. 11 **a** Time series of precipitation rates (mm/day) averaged over the global dry regions (see Fig. 1) during the local summer monsoon season (MJJAS in NH and NDJFM in SH). The dashed line indicates the corresponding linear trend, which is significant at 95% confidence level by both the MK and trend-to-noise ratio tests. **b** The same as in **a** except for the NH dry regions with the trend significant at 90% confidence level. For comparison, global and NH monsoon precipitation (scale on the right) along with their trends shown in Fig. 6a are plotted in gray lines in **a** and **b**, respectively



We also found that the intensification of the annual cycle of the earth’s climate system over the past 30 years is due primarily to the enhanced GMP, especially the NHSM (Figs. 4, 5). This poses a statistical perspective for climate

models that are used to predict decadal variation and near-term projection planned for the IPCC Fifth assessment.

The intensification of the GMP originates primarily from an enhanced east–west thermal contrast in the Pacific

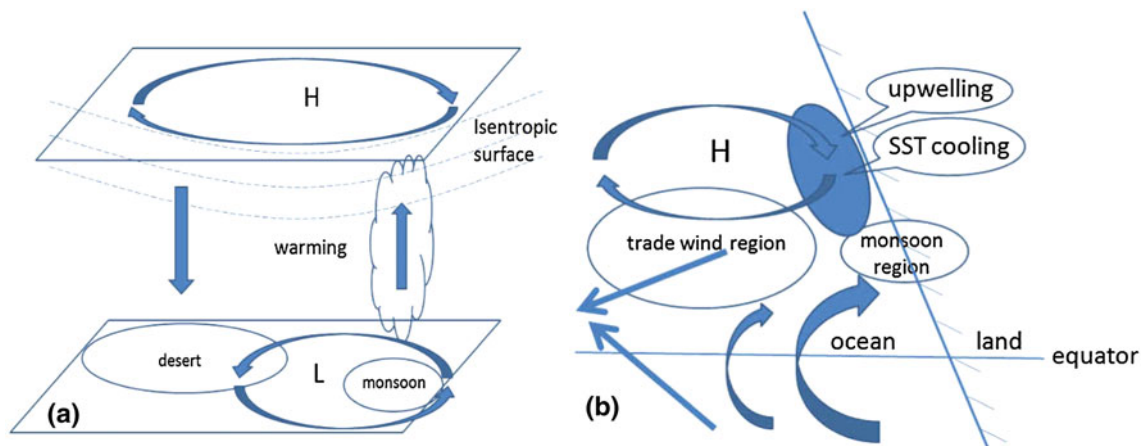


Fig. 12 Schematic diagram showing monsoon-desert coupling mechanism. **a** Descending motion induced by monsoon-westerly interaction. **b** Enhancement of the monsoon-subtropical high coupling by air-sea interaction over the oceanic subtropical high

Ocean, which is coupled with a rising pressure in the EP and decreasing pressure over the Indo-Pacific warm pool. This enhanced Pacific zonal thermal contrast tends to amplify both NHSM and SHSM. The enhanced Pacific zonal thermal contrast is largely a result of natural variability, i.e., the IPO.

Over the past three decades, the NHSM has a significant upward trend, while the SHSM trend is relatively weak. This difference cannot be explained by the east-west thermal contrast trend which is symmetric about the equator. Rather, it is caused by the relatively large warming trend in the NH, which creates a hemispheric thermal contrast that favors intensification of the NHSM but weakens the SHSM. The enhanced hemispherical thermal contrast is likely due to anthropogenic forcing.

We have shown that the wet-get-wetter and dry-gets-drier precipitation trend over the past 30 years is likely a result of the intensifying global summer monsoon precipitation (Figs. 10, 11) through a monsoon-desert coupling mechanism (Fig. 12). While this trend bears similarity to the precipitation trend pattern projected by the majority of the global climate models under increasing anthropogenic forcing, we should note that the observed “wet-gets-wetter” pattern is associated with enhanced Walker circulation, while the similar pattern found in the future projections is associated with weakening Walker circulation and mainly caused by increased water vapor (Rodwell and Hoskins 2001; Held and Soden 2006).

The findings described here are helpful in determining what may have occurred to the GM during the last period of secular warming in the mid-twentieth century (Polyakov et al. 2003). Furthermore, a comparison of the GM in the most recent period of warming with the mid-twentieth century warming may help determine the proportion of climate change that is attributable to anthropogenic effects

and that is a part of long-term internal variability of the complex climate systems.

Acknowledgments This work is supported by US NSF award #AGS-1005599 (BW) and NSF-ATM 0965610 (PJW), the National Research Programs of China (Award Nos. XDA05080800, 2010CB950102, 2011CB403301 and 2010CB833404) (JL and BW), and Environment Research and Technology Development Fund (A0902) of the Japanese Ministry of the Environment (HJK). BW and HJK acknowledge support from the International Pacific Research Center which is funded jointly by JAMSTEC, NOAA, and NASA. This is publication no. 8535 of the School of Ocean and Earth Science and Technology and publication no. 837 of the International Pacific Research Center.

Open Access This article is distributed under the terms of the Creative Commons Attribution Noncommercial License which permits any noncommercial use, distribution, and reproduction in any medium, provided the original author(s) and source are credited.

References

- Anderson DLT, Gill AE (1975) Spin-up of a stratified ocean, with application to upwelling. *Deep Sea Res* 22:583–596
- Biasutti M, Battisti DS, Sarachik ES (2003) The annual cycle over the tropical Atlantic, South America, and Africa. *J Clim* 16:2491–2508
- Chou C, Tu JY, Tan PH (2007) Asymmetry of tropical precipitation change under global warming. *Geophys Res Lett* 34:L17708. doi:10.1029/2007GL030327
- Deser C, Phillips AS, Hurrell JW (2004) Pacific interdecadal climate variability: linkages between the tropics and the North Pacific during boreal winter since 1900. *J Clim* 17:3109–3124
- Ding QH, Wang B, Wallace M, Branstator G (2011) Tropical-extratropical teleconnections in boreal summer: observed inter-annual variability. *J Clim* 24:1878–1896
- Dore MHI (2005) Climate change and changes in global precipitation patterns: what do we know? *Environ Int* 31:1167–1181
- Enfield DB (1996) Relationships of inter-American rainfall to tropical Atlantic and Pacific SST variability. *Geophys Res Lett* 23:3305–3308

- Held IM, Soden BJ (2006) Robust responses of the hydrological cycle to global warming. *J Clim* 19:5686–5699
- Higgins RW, Douglas A, Hannmann A et al (2003) Progress in Pan American CLIVAR research: the North American monsoon system. *Atmosfera* 16:29–65
- Hoskins BJ (1996) On the existence and strength of the summer subtropical anticyclones. *Bull Am Meteorol Soc* 77:1287–1291
- Hoskins BJ, Wang B (2006) Large scale atmospheric dynamics. In: Wang B (ed) *The Asian monsoon*. Springer-Praxis, Berlin, pp 357–416
- Huffman GJ, Adler RF, Bolvin DT, Gu G (2009) Improving the global precipitation record: GPCP Version 2.1. *Geophys Res Lett* 36:L17808. doi:[10.1029/2009GL040000](https://doi.org/10.1029/2009GL040000)
- Kanamitsu M, Ebisuzaki W, Woollen J, Yang SK, Hnilo JJ, Fiorino M, Potter GL (2002) NCEP-DOE AMIP-II reanalysis (R-2). *Bull Am Meteorol Soc* 83:1631–1643
- Kendall MG (1955) *Rank correlation methods*. Charles Griffin & Co., London
- Kutzbach JE, Otto-Bliesner BL (1982) The sensitivity of the African-Asian monsoonal climate to orbital parameter changes for 9000 yr B.P. in a low-resolution general circulation model. *J Atmos Sci* 39:1177–1188
- Lau KM, Weng H (2002) Recurrent teleconnection patterns linking summertime precipitation variability over East Asia and North America. *J Meteorol Soc Jpn* 80:1309–1324
- Liu Z, Harrison SP, Kutzbach JE, Otto-Bliesner B (2004) Global monsoons in the mid-Holocene and oceanic feedback. *Clim Dyn* 22:157–182
- Liu J, Wang B, Ding Q et al (2009) Centennial variations of the global monsoon precipitation in the last millennium: results from ECHO-G model. *J Clim* 22:2356–2371
- Loschnigg J, Webster PJ (2000) A coupled ocean–atmosphere system of SST regulation for the Indian Ocean. *J Clim* 13:3342–3360
- McBride JL (1987) The Australian summer monsoon. In: Chang C-P, Krishnamurti TN (eds) *Monsoon meteorology*. Oxford University Press, Oxford, pp 203–231
- Meehl GA (1987) The annual cycle and interannual variability in the tropical Pacific and Indian Ocean regions. *Mon Weather Rev* 115:27–50
- Meehl GA, Stocker TF, Collins WD, Friedlingstein P, Gaye AT, Gregory JM, Kitoh A, Knutti R, Murphy JM, Noda A, Raper SCB, Watterson IG, Weaver AJ, Zhao Z-C (2007) Global climate projections. In: Solomon S, Qin D, Manning M, Chen Z, Marquis M, Averyt KB, Tignor M, Miller HL (eds) *Climate change 2007: the physical science basis*. Contribution of working group I to the fourth assessment report of the Intergovernmental Panel on Climate Change. Cambridge University Press, Cambridge
- Neelin JD, Held IM (1987) Modeling tropical convergence based on the moist static energy budget. *Mon Weather Rev* 115:3–12
- Neelin JD et al (2006) Tropical drying trends in global warming models and observations. *Proc Natl Acad Sci* 103:6110–6115
- Nicholson SE, Kim E (1997) The relationship of the El Niño Southern oscillation to African rainfall. *Int J Climatol* 17:117–135
- Polyakov IV, Bekryaev RV, Alekseev GV, Bhatt US, Colony RL, Johnson MA, Maskshitas AP, Walsh D (2003) Variability and trends in air temperature and pressure in the maritime Arctic. *J Clim* 16:2067–2077
- Power S, Casey T, Folland CK, Colman A, Mehta V (1999) Interdecadal modulation of the impact of ENSO on Australia. *Clim Dyn* 15:319–323
- Ramage CS (1971) *Monsoon meteorology* (Int Geophys Ser, vol 15). Academic Press, San Diego
- Rasmussen EM, Carpenter TH (1982) Variations in the tropical sea surface temperature and surface wind fields associated with the Southern Oscillation/El Niño. *Mon Weather Rev* 110:354–384
- Rodwell MJ, Hoskins BJ (2001) Subtropical anticyclones and summer monsoon. *J Clim* 14:3192–3211
- Smith TM, Reynolds RW, Peterson TC, Lawrimore J (2008) Improvements to NOAA’s historical merged land-ocean surface temperature analysis (1880–2006). *J Clim* 21:2283–2296
- Tao S, Chen L (1987) A review of recent research on the East Asian summer monsoon in China. In: Chang C-P, Krishnamurti TN (eds) *Monsoon meteorology*. Oxford University Press, Oxford, pp 60–92
- Trenberth KE, Stepaniak DP, Caron JM (2000) The global monsoon as seen through the divergent atmospheric circulation. *J Clim* 13:3969–3993
- Uppala SM, Kallberg PW, Simmons AJ, Andrae U, da Costa Bechtold V, Fiorino M, Gibson JK, Haseler J, Hernandez A, Kelly GA, Li X (2005) The ERA-40 reanalysis. *Q J R Meteorol Soc* 131:2961–3012
- Wallace JM, Smith C, Bretherton CS (1992) Singular value decomposition of wintertime sea surface temperature and 500-mb height anomalies. *J Clim* 5:561–576
- Wang B, Ding QH (2006) Changes in global monsoon precipitation over the past 56 years. *Geophys Res Lett* 33:L06711. doi:[10.1029/2005GL025347](https://doi.org/10.1029/2005GL025347)
- Wang B, Ding QH (2008) Global monsoon: dominant mode of annual variation in the tropics. *Dyn Atmos Oceans* 44:165–183
- Wang B, Wu R, Lau KM (2001) Interannual variability of Asian summer monsoon: contrast between the Indian and western North Pacific-East Asian monsoons. *J Clim* 14:4073–4090
- Wang B, Wu R, Li T (2003) Atmosphere–warm ocean interaction and its impact on Asian-Australian monsoon variation. *J Clim* 16:1195–1211
- Wara MW, Ravelo AC, Delaney ML (2005) Permanent El Niño-like conditions during the Pliocene warm period. *Science* 309:758–761
- Webster PJ, Magana VO, Palmer TN, Shukla J, Tomas RA, Yanai M, Yasunari T (1998) Monsoons: processes, predictability, and the prospects for prediction. *J Geophys Res* 103:14451–14510
- Wentz FJ, Ricciardulli L, Hilburn K, Mears C (2007) How much more rain will global warming bring? *Science* 317:233–235
- Xie P, Arkin PA (1997) Global precipitation: a 17-year monthly analysis based on gauge observations, satellite estimates, and numerical model outputs. *Bull Am Meteorol Soc* 78:2539–2558
- Yin P, Gruber A, Arkin P (2004) Comparison of the GPCP and CMAP merged gauge-satellite monthly precipitation products for the period 1979–2001. *J Hydrometeorol* 5:1207–1222
- Zhang X, Zwiers FW, Hegerl GC, Lambert FH, Gilett NP, Solomon S, Stott PA, Nozawa T (2007) Detection of human influence on twentieth-century precipitation trends. *Nature* 448:461–465
- Zhou JY, Lau KM (1998) Does a monsoon climate exist over South America? *J Clim* 11:1020–1040